



Modeling, Simulation and Analysis of Doubly-Fed Induction Generator for Wind Turbines Under Grid Voltage Fluctuation

Karrar M. Al-Anbary¹ Hayder Hussein Kadhum² Abdulrasul.A.Al-hayder³

1,2,3 Department of Electrical Engineering, University of Babylon

Karrar139@yahoo.com eng.hayder.kadhum@uobabylon.edu.iq Ajwadi.haydari@gmail.com

Corresponding Author : eng.hayder.kadhum@uobabylon.edu.iq

Received:	20/6/2021	Accepted:	10/11/2021	Published:	28/11/2021
-----------	-----------	-----------	------------	------------	------------

Abstract:

To ensure the best operations situation of the wind turbine under critical conditions, a thoroughly analysis of converter controls in both machine and grid sides is essential. The grid side is playing the major role therefore its codes as stabilization, fault ride through, quality of power improving, synchronizing, controlling power and other codes must be satisfied. This paper aims to analyze the Doubly-Fed Induction Generator (DFIG). Analysis shall cover the situations: under balanced grid, under voltage sag, under voltage swell, under changes in reactive power demand and under changes in supply frequency. The system model and controlling are needed to analyze the whole DFIG system in the steady-state and transient state operations. A back to back converters are used in this system. A model of the grid converter independently controlling the active and reactive power including dc-link voltage is constructed. Machine side converter model is also built such that it is maintaining the unity power-factor and controlling reactive power regardless the transient condition of the grid. MATLAB/SIMULINK models are used for this analysis.

Key words: Doubly-Fed Induction Generator (DFIG), Modeling, Simulation and Analysis

1.Introduction

Kyoto protocol and other summits concerning the “climate changes” have issued a real warning of the negative effects of science speedy progress on the environment. Electricity, which is the first source of energy needed is also the main source of the environmental pollution because of the fuel type used to generate, which is mainly a coal-like fuel. A renewable energy source is becoming one of the most interesting issues for the scientific and industrial communities. A hydel and a wind-borne electricity are avenues of producing clean electrical energy. Electrical machine as a generator is used to produce the electricity. Induction machine, with its noticeable positive criteria comparing to synchronous and DC generator, is becoming the preferable machine type for this purpose. Doubly Fed Induction Generator (DFIG) which is a “Wound Rotor machine” is becoming essential in the wind farms and hydel (from stand-alone to the grid connected). The grid side converter is a key part to ensure the wind turbine grid code necessities [1].

The grid power (active and reactive) could be independently controlled by the line side converter’s vector control [2,3] is explaining the energy recovery of DFIG with controlled and a variable frequency at the rotor side. A current controlled cyclo-converter was used by [4] to analyze the DFIG steady state analysis behavior. The wind-turbine optimum torque speed contour is traced for DFIG system which is a stator field oriented controlled [5]. The equilibrium state of a 3-phase grid was analyzed in [6,7] when a grid converter is controlled by VOC (Voltage Oriented Control). This work is studying and analyzing the DFIG system at different cases of grid voltage fluctuations.

Most the researches dealing with the DFIG wind turbine controlling techniques in [8,9] are concentrating on how to possibly supply all the power generated to the grid economically. To be able to reach this situation, the wind turbine must be operated in a varied range of the speed of wind within the rated ranges of power and produced voltage as well as the specified power-factor. However, the nowadays is requiring the wind turbine to adjust the re-active and active powers corresponding to the power setting power points of the system controller which are take in to consideration the ability of power producing besides the needed power. This paper is focusing on studying the controlling of the DFIG wind turbine to serve this purpose. The turbine blades are the part which is responsible for

collecting the kinetic energy from the wind. Therefore there are many trials to design the blade [10-12] to be optimally collecting the wind energy. The profile is depending on the blade shape including the rotation and the tip angle. The simplicity of the design of turbine rotor is a general practice considering the theoretical optimality and the practical ability of construction [13].

The following DFIG's categories are the reasons behind its use in this study:

- Its capability of reactive power controlling and decoupling it from active power controlling by controlling the current of the rotor excitation independently.
- The magnetization of DFIG could be done from the rotor circuit and not only from the grid. It is also able to provide the stator with the power by its reactive power through the converter of the grid side.
- If the grid voltage fluctuated the DFIG could be in the case of a weak grid, where the voltage may fluctuate, the DFIG may be organized to control the voltage grid by producing or absorbing the needed voltage.

This paper is also considering the fluctuations of the grid voltage in the DFIG system analyses.

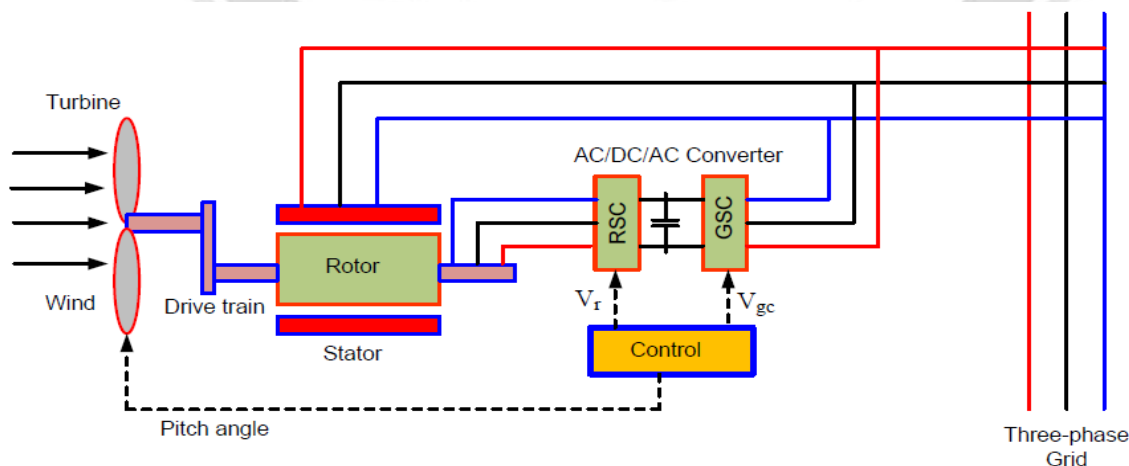
2. Doubly-Fed Induction Generator (DFIG) System

DFIG is an induction machine with two back-to-back converters. The machine's stator is connected to the grid through one of the two converters. The other converter is connected to the rotor of the machine via a DC-link capacitor. The function of the converter in the grid side is to keep the DC-link voltage constant. The machine side converter is regulating the prime mover speed which is giving the system the ability to be normally functioning with variable speeds.

The d-q reference frame model was constructed for both the steady and transient states of DFIG. The rotor d-q currents and the references of the stator real/reactive power in a determined orientation relation is clarified using the steady-state model. The power controlling of DFIG directives are acquired through the transient model. Figure (1) is showing the whole system blocks.

The main parts of the system are:

1. PWM Voltage source converters (Grid side converter and Machine side converter)
2. Utility grid
3. PI controller



Fig(1) basic diagram of Doubly fed induction generator with converters



3. Dynamic Modeling of DFIG in State Space Equations

Each dynamic system could be represented in space of “n” co-ordinate axes where “n” is the number of system’s function of time states. This representation is called the state space representation which could be simulated as a model by using MatLab. This representation and modeling is of a great help in analyzing the transient behavior of the system. The state space equations fundamentals are, Equations (1) are the general forms of the linear time invariant system state-space representation where A, B, C and D are constant matrices. Eq. (1) - (11) are the state space model of DFIG model (Ψ_{qs} , Ψ_{ds} , Ψ_{qr} , Ψ_{dr} are the state variables) [8].

$$\begin{cases} X(t) = AX(t) + BU(t) \\ Y(t) = CX(t) + DU(t) \end{cases} \quad (1)$$

Equations (2) are for linear time variant system, where A, B, C, D are time dependent matrices.

$$\begin{cases} X(t) = A(t)X(t) + B(t)U(t) \\ Y(t) = C(t)X(t) + D(t)U(t) \end{cases} \quad (2)$$

The synchronously rotating frame (having flux linkages as the state variables) DFIG machine’s state space representation is as in Equations (3) represent the voltage and flux equations).

$$\begin{aligned} V_{qs} &= R_s i_{qs} + \frac{1}{\omega_b} \frac{d}{dt} \Psi_{qs} + \frac{\omega_e}{\omega_b} \Psi_{dr} \\ V_{ds} &= R_s i_{ds} + \frac{1}{\omega_b} \frac{d}{dt} \Psi_{ds} + \frac{\omega_e}{\omega_b} \Psi_{qs} \\ V_{qr} &= R_r i_{qr} + \frac{1}{\omega_b} \frac{d}{dt} \Psi_{qr} + \frac{(\omega_e - \omega_r)}{\omega_b} \Psi_{dr} \\ V_{dr} &= R_r i_{dr} + \frac{1}{\omega_b} \frac{d}{dt} \Psi_{dr} + \frac{(\omega_e - \omega_r)}{\omega_b} \Psi_{qr} \end{aligned} \quad (3)$$

The set of Equations(4) is modeling the flux linkage in terms of reactance.

$$\begin{aligned} \Psi_{qs} &= X_{Is} i_{qs} + X_m (i_{qs} + i_{qr}) \\ \Psi_{ds} &= X_{Is} i_{ds} + X_m (i_{ds} + i_{dr}) \\ \Psi_{qr} &= X_{Is} i_{qr} + X_m (i_{qs} + i_{qr}) \\ \Psi_{dr} &= X_{Ir} i_{dr} + X_m (i_{ds} + i_{dr}) \\ \Psi_{qm} &= X_m (i_{qs} + i_{qr}) \\ \Psi_{dm} &= X_m (i_{ds} + i_{dr}) \end{aligned} \quad (4)$$



The currents in terms of flux linkages and mutual flux linkages (ψ_{qm} and ψ_{dm}) are as in Equations (5)

$$\left. \begin{aligned} i_{qs} &= \frac{\psi_{qs} - \psi_{qm}}{X_{Is}} \\ i_{qr} &= \frac{\psi_{qr} - \psi_{qm}}{X_{Ir}} \\ i_{ds} &= \frac{\psi_{ds} - \psi_{dm}}{X_{Is}} \\ i_{dr} &= \frac{\psi_{dr} - \psi_{dm}}{X_{Ir}} \end{aligned} \right\} \quad (5)$$

The voltages in terms of currents can be expressed:

$$\left. \begin{aligned} V_{qs} &= \frac{R_s}{X_{Is}} (\psi_{qs} - \psi_{qm}) + \frac{1}{\omega_b} \frac{d\psi_{qs}}{dt} + \frac{\omega_e}{\omega_b} \psi_{ds} \\ V_{ds} &= \frac{R_s}{X_{Is}} (\psi_{ds} - \psi_{dm}) + \frac{1}{\omega_b} \frac{d\psi_{ds}}{dt} - \frac{\omega_e}{\omega_b} \psi_{qs} \\ V_{qs} &= \frac{R_s}{X_{Is}} (\psi_{qs} - \psi_{qm}) + \frac{1}{\omega_b} \frac{d\psi_{qs}}{dt} + \frac{\omega_e}{\omega_b} \psi_{ds} \\ V_{qr} &= \frac{R_r}{X_{Ir}} (\psi_{qr} - \psi_{qm}) + \frac{1}{\omega_b} \frac{d\psi_{qr}}{dt} + \frac{(\omega_e - \omega_r)}{\omega_b} \psi_{dr} \end{aligned} \right\} \quad (6)$$

The DFIG state variables can be deduced from (6) as in Equations set (7).

$$\left. \begin{aligned} \frac{d\psi_{qs}}{dt} &= \omega_b \left[V_{qs} - \frac{\omega_e}{\omega_b} \psi_{ds} - \frac{R_s}{X_{Is}} (\psi_{qs} - \psi_{qm}) \right] \\ \frac{d\psi_{ds}}{dt} &= \omega_b \left[V_{ds} - \frac{\omega_e}{\omega_b} \psi_{qs} - \frac{R_s}{X_{Is}} (\psi_{ds} - \psi_{dm}) \right] \\ \frac{d\psi_{qr}}{dt} &= \omega_b \left[V_{qr} - \frac{R_r}{X_{Ir}} (\psi_{qr} - \psi_{qm}) - \left(\frac{\omega_e - \omega_r}{\omega_b} \right) \psi_{dr} \right] \\ \frac{d\psi_{dr}}{dt} &= \omega_b \left[V_{dr} - \frac{R_r}{X_{Ir}} (\psi_{dr} - \psi_{dm}) + \left(\frac{\omega_e - \omega_r}{\omega_b} \right) \psi_{qr} \right] \end{aligned} \right\} \quad (7)$$

where

$$\left. \begin{aligned} \psi_{qm} &= \frac{X_{ml}}{X_{Is}} \psi_{qs} + \frac{X_{ml}}{X_{Ir}} \psi_{qr} \\ \psi_{dm} &= \frac{X_{ml}}{X_{Is}} \psi_{ds} + \frac{X_{ml}}{X_{Ir}} \psi_{dr} \\ X_{ml} &= \left(\frac{X_m X_{Is} X_{Ir}}{X_{Is} X_{Ir} + X_m X_{Ir} + X_m X_{Is}} \right) \end{aligned} \right\} \quad (8)$$

The state space matrix shall be as in Eq (9).

$$\begin{bmatrix} \dot{\psi}_{qs} \\ \dot{\psi}_{ds} \\ \dot{\psi}_{qr} \\ \dot{\psi}_{dr} \end{bmatrix} = \begin{bmatrix} \frac{R_s}{X_{ls}} & \frac{\omega_e}{\omega_b} & 0 & 0 \\ \frac{\omega_e}{\omega_b} & -\frac{R_s}{X_{ls}} & 0 & 0 \\ 0 & 0 & -\frac{R_r}{X_{lr}} & -\frac{(\omega_e - \omega_r)}{\omega_b} \\ 0 & 0 & \frac{(\omega_e - \omega_r)}{\omega_b} & -\frac{R_r}{X_{lr}} \end{bmatrix} \begin{bmatrix} \psi_{qs} \\ \psi_{ds} \\ \psi_{qr} \\ \psi_{dr} \end{bmatrix} + \begin{bmatrix} 1 & 0 & 0 & 0 \\ 0 & 1 & 0 & 0 \\ 0 & 0 & 1 & 0 \\ 0 & 0 & 0 & 1 \end{bmatrix} \begin{bmatrix} v_{qs} \\ v_{ds} \\ v_{qr} \\ v_{dr} \end{bmatrix} + \begin{bmatrix} \frac{R_s}{X_{ls}} & 0 \\ 0 & \frac{R_s}{X_{ls}} \\ \frac{R_r}{X_{lr}} & 0 \\ 0 & \frac{R_r}{X_{lr}} \end{bmatrix} \begin{bmatrix} \psi_{qm} \\ \psi_{dm} \end{bmatrix} \quad (9)$$

The electromotive torque is generated due to the mutual effects of rotor's mmf and the flux of the air-gap. The rotor is not moving at the synchronous speed and therefore no emf generated so no current as well and this makes the torque be zero. At any other none-synchronous speed, torque will be produced and hence the machine shall behave as a motor. When machine used as a generator the torque is provided by a mean of mechanical movement which could be provided by wind (which is the case in this work). Torque equations in terms of current and flux linkages could be written as in Equation(10).

$$\begin{aligned} T_e &= \frac{3P}{2} (\lambda_{ds} i_{qs} - \lambda_{qs} i_{ds}) \\ &= \frac{3P}{2} (i_{qs} i_{qr} - i_{ds} i_{dr}) \\ &= \frac{3P}{2} (\lambda_{dr} i_{qr} - \lambda_{dr} i_{dr}) \end{aligned} \quad (10)$$

Torque equations in terms of state variables as:

$$\begin{aligned} T_e &= \frac{3P}{2} \frac{1}{\omega_b} (\Psi_{ds} i_{qs} - \Psi_{qs} i_{ds}) \\ &= \frac{3P}{2} \frac{1}{\omega_b} (\Psi_{dr} i_{qr} - \Psi_{qr} i_{dr}) \end{aligned} \quad (11)$$

4. Grid Side Converter Control

The grid side converter is used to regulate the voltage of the DC link between the two converters. The unexpectedly changes of the grid voltage as a result of the sudden load changes and/or abrupt changes of the wind speed which is causing changes across the rotor and stator of the DFIG. The back-to-back converters and the dc-link capacitor shall also have the same effects. The grid voltage and the DFIG stator voltage are same because grid is directly connected to the DFIG, this means that the DC link voltage is related to the grid voltage. there is a relationship between the grid voltage and the DC link voltage. The mathematical model in equations (12) are clarifying the grid side converter voltages [8].



$$\begin{cases} V_d = R i_d + L \frac{di_d}{dt} - \omega_e L i_q + V_{d1} \\ V_q = R i_q + L \frac{di_q}{dt} + \omega_e L i_d + V_{q1} \end{cases} \quad (12)$$

v_{d1} and v_{q1} are the two-phase voltages found from v_a , v_b and v_c using d-q theory. The settings of the reference values are setting such that the DC link voltage is constant and a unity power factor of the complete system. The grid side converters reference voltage vectors are found Eq(13).

$$\begin{cases} V_d^* = V_d - i_d^* R + i_q^* \omega_e L - V_d \\ V_q^* = V_q - i_q^* R + i_d^* \omega_e L - V_d \end{cases} \quad (13)$$

The plants for the voltage and current loops are shown in Eq. (14) below.

$$\begin{cases} F(s) = \frac{i_d(s)}{V_d(s)} = \frac{i_q(s)}{V_q(s)} = \frac{1}{L_s + R} \\ G(s) = \frac{V_{ds}(s)}{i_d(s)} = \frac{3m_1}{2\sqrt{2}} \end{cases} \quad (14)$$

The controlling of active and reactive power is established independently by dq current component that administered by (15). Figure (2) is showing the detail control policy.

$$\begin{cases} P_s = \frac{3}{2} (V_d i_d + V_q i_q) \\ Q_s = \frac{3}{2} (V_d i_q - V_q i_d) \end{cases} \quad (15)$$

5. Machine Side Converter Control

The goal of the converter at the machine piece Figure 2 is to control the speed of the rotor to keep it constant even with the changes of the wind speed. The other purpose of the converter is controlling the active and reactive power stream by the current of the rotor. The two types of power (active and reactive) flow are controlled by the two components of the rotor current, i_{dr} is controlling the active while i_{qr} is to control the reactive. The reactive power value must be zero to get a unity power factor. The unit vector is found in the same method that is used in the grid side converter case. The next equations are the machine side converter mathematical model. The reference voltage vectors for machine side converter are being derived using Eq (16).

$$\begin{aligned}
 V_{dr}^* &= V_{dr} + i_{dr}R_r - (\omega - \omega_r)[i_{qr}L_r + L_m i_{qs}] \\
 V_{qr}^* &= V_{qr} + i_{qr}R_r + (\omega - \omega_r)[i_{dr}L_r + L_m i_{ds}] \\
 V_{dr}^* &= V_{dr} + i_{dr}R_r - (\omega - \omega_r)[i_{qr}L_r + L_m i_{qs}] \\
 V_{qr}^* &= V_{qr} + i_{qr}R_r + (\omega - \omega_r)[i_{dr}L_r + L_m i_{ds}]
 \end{aligned}
 \tag{16}$$

Where V_{dr} and V_{qr} are determined by feeding the current errors to a standard PI controller. The reference input current i_{dr}^* could be deduced from reference torque Equ(17) or from the speed error in the speed control using standard PI controller. In the same way the reactive power errors is used to find i_{qr}^* . Current control loops are controlled by speed and reactive power. The following expression is to calculate the electromagnetic torque.

$$\begin{aligned}
 T_e &= \frac{3}{2} \frac{P}{2} (\lambda_{ds} i_{qs} - \lambda_{qs} i_{ds}) \\
 &= -\frac{3}{2} \frac{P}{2} \lambda_{qs} i_{ds} \\
 &= -\frac{3}{2} \frac{P}{2} \lambda_{qs} \left[-\frac{L_m}{L_s} i_{dr} \right] \\
 &= \frac{3}{2} \frac{P L_m}{2 L_s} \lambda_{qs} i_{dr}
 \end{aligned}
 \tag{17}$$

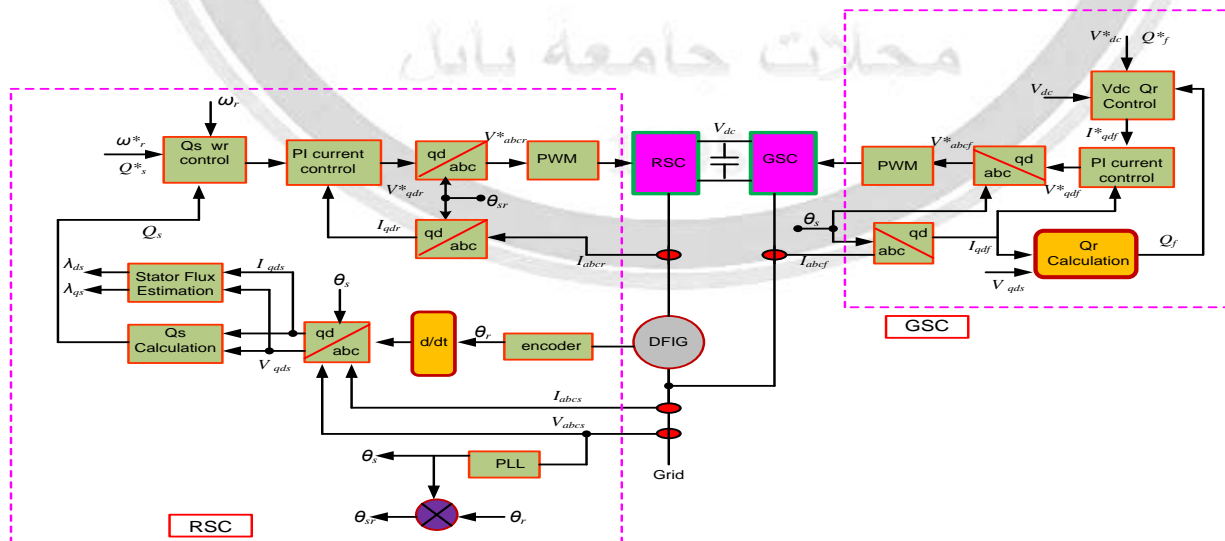


Fig (2) Schematic diagram of DFIG wind turbine Control Structure



6. Basic Concepts and Aerodynamic Characteristics of the Wind Turbine

The mechanical power is produced from the wind kinetic energy by a transducer called “wind turbine”. The wind kinetic energy depends on the wind speed and the density of air as in Equations (18). [13]

$$P_{\text{air}} = \frac{1}{2} (\text{air mass per unit time})(\text{wind velocity})^2$$

$$P_{\text{air}} = \frac{1}{2} \pi \rho R^2 v^3 \quad (18)$$

ρ : is the air density (1.225 kg/m³) and V is the wind velocity

R : radius of the rotor or the blade length [m]

Practically, the wind kinetic energy couldn't be transformed into mechanical energy. Therefore, the power captured from the wind turbine is obtained as follows [14, 15]: power coefficient, C_p used to describe the performance of any size of wind turbine rotor.

$$C_p = \frac{P_{\text{wind turbine}}}{P_{\text{air}}} \quad (19)$$

$$P_w = \frac{1}{2} C_p(\lambda, \beta) \pi \rho R^2 v^3 \quad (20)$$

Theoretically the maximum achievable power factor coefficient never more than 59.3% (Betz limit) while in practice it can reach to 45% [13] which is below the theoretical limit due to inefficiencies and losses related to different configurations of airfoil profile. The relationship between the wind speed and the rate of rotation of the rotor is no dimensional factor named the tip speed ratio (TSR) λ which is described as follows:

$$\lambda = \frac{\text{blade tip speed}}{\text{wind speed}} \quad (21)$$

Equation (22) is to calculate the tip speed of the blade as a function of the turbine rotational speed and blades' length.

$$\text{blade tip speed} = \frac{\text{rotational speed (rpm)} * \pi * D}{60} \quad (22)$$

Where D is turbine diameter

The different mathematical formulae have been used in previous studies to calculate the power coefficient and one of these is shown below [11]:

$$C_p(\lambda, \beta) = C_1(C_2 - C_3\beta - C_4)e^{-C_5} + 0.0085\lambda \quad (23)$$

Where:

$$\lambda_i = \frac{1}{\lambda - 0.08\beta} - \frac{0.035}{1 + \beta^3}$$

$$C_1 = 0.5872, \quad C_2 = \frac{116}{\lambda_i}, \quad C_3 = 0.4, \quad C_4 = 5, \quad C_5 = \frac{21}{\lambda_i}$$



7. Wind Turbines' Standard Features'

The following paragraphs are graphically explanation of the wind turbine performance at various wind speeds.

7.1. Power versus Speed behavior

Figure (3) is showing the performance of the turbine at various wind speeds [14]. Fig (4) is showing changes in the coefficient of power according to TSR (λ) with a controlled pitch of blade (the power coefficient depends not only on TSR but also on the blade pitch angle).the C_p is maximum while increasing the pitch angle the power coefficient decreases. (At $\beta=0$, the value of C_p is maximum this value reduces as the pitch angle increases. This is the important fact to be considered when pitching the turbine blades).

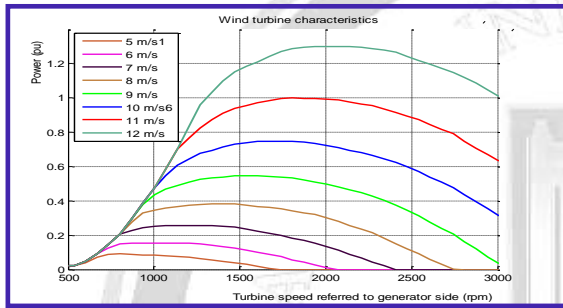


Fig (3) the power-speed curves of wind turbine

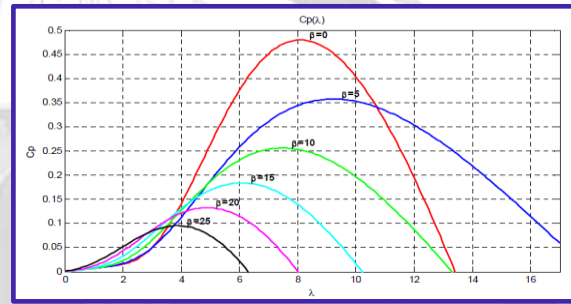


Figure (4): Power coefficient for different pitch angles

Typical characteristic of the power coefficient with respect to the tip speed ratio (TSR λ) and blade pitch control in Figure [5] it can reach to 48% .

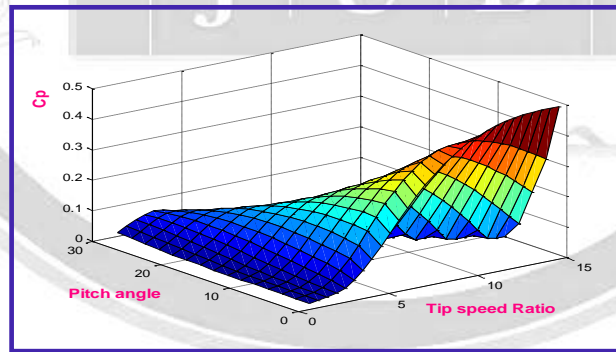


Figure (5): Power coefficient versus pitch angles and tip-speed-ratios

7.2. Torque-Speed Curves

The rotational speed of the torque-shaft curves for several wind speeds are in figure (6). It is showing that for each wind speed there is one rotational speed producing maximum torque (T_{max}) which is having a contour as a function of the square of the shaft radial speed (ω^2). When electricity produced, the electrical load is affecting the torque. By proper choose of this load, the torque could be made to be changing with the square of the shaft radial speed. Equation (21) is showing this relationship.

www.journalofbabylon.com

ISSN: 2616 - 9916

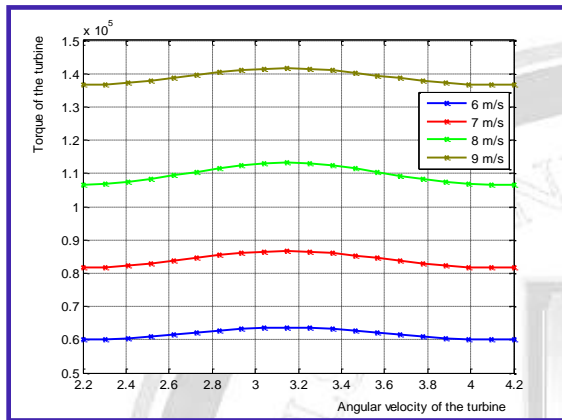
www.journalofbabylon.com

Journal.eng@uobabylon.edu.iq

info@journalofbabylon.com

Tabal-1(Rating and Specification of DFIG). The wind turbine in this study is on 1.5MW, with a horizontal axis, and three-bladed with blade radius 35m, wind turbine with pitch control. A DFIG of two-pair pole is used. The parameters of the DFIG based wind turbine system. Table 1 is stating these parameters which are close to the wind turbine that are commercially available. Figure (7) shows the structure of the grid-synchronization DFIG system completely with a converter mode.

Table(1)



Rated Power	10hp
Stator Voltage	415V
Rs(Stator Resistance)	1.11Ω
Rr(Rotor Resistance)	0.9Ω
Ls (Stator Inductance)	0.3H
Lm(Mutual inductance)	0.08H(Referred to the rotor)
Lr (Rotor inductance)	0.09H(Referred to the rotor)
Poles	6
Rated speed	1100 rpm
DC link Voltage	850V
Switching Frequency of IGBTs	3kHz
Dc link capacitor	10000μF
Air density	2.25:Kg/m ³
Sweap area Reads	35m
Gearbox ratio	90

Fig (6). The torque versus speed characteristics of wind turbine

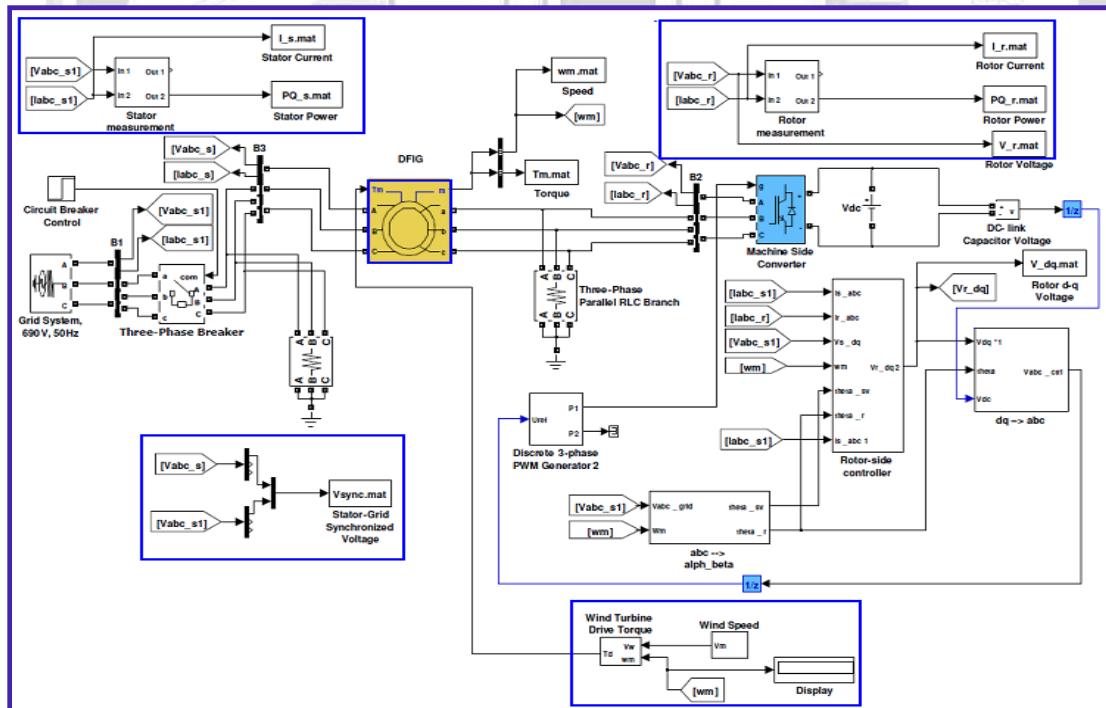


Figure (7): The DFIG wind turbine model test system under Matlab/SimPower System

The speed of the rotor is controlled using the PID type in the model of the system. PID controller is adjusting the pitch angle of the blade to keep the rotor speed constant regardless of the wind speed changes. Figure 6 illustrate the controller behavior where $\Delta\omega_r$ (input) is the rotor speed changes and ΔU_c is the pitch angle changes (out-put) operation of the controller where represents the variations in the rotor speed and represents the changes in the output .Figure 8 shows the closed loop system using the rotor current control (RSC in S-domain) using PI controller which is commonly and effectively used in automatically controlled systems. The controller could also be used to guard the DFIG system from the over-current damages by using a current limiters in the loop as shown below. Figure 9 shown (T_s), is the sample time 0.5ms. The control of the current in RSC in z-domain. Figure (10) shows The control of the current in the GSC have parameters used in the standard design techniques of the DFIG system may be applied

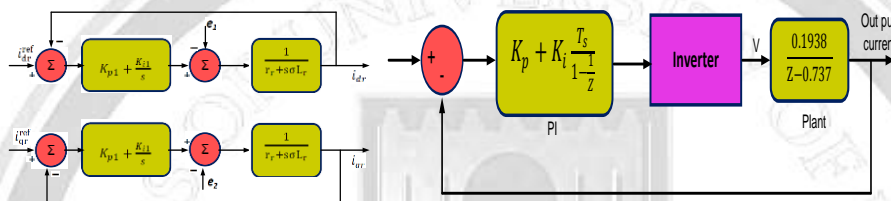


Figure (8): Closed loop current control of RSC in S-domain

Figure (9). control of the current in RSC in z-domain

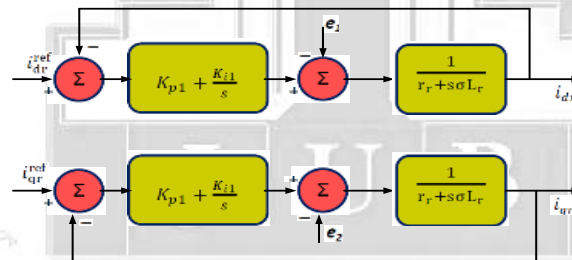


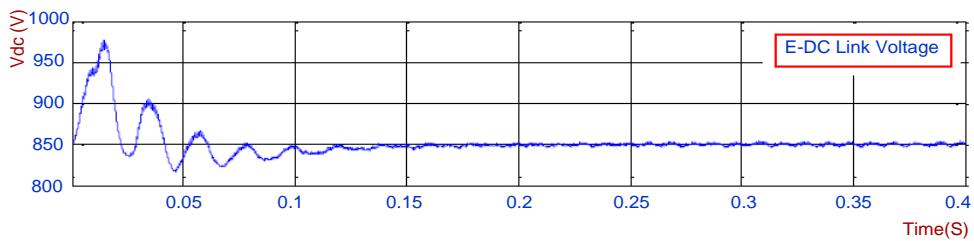
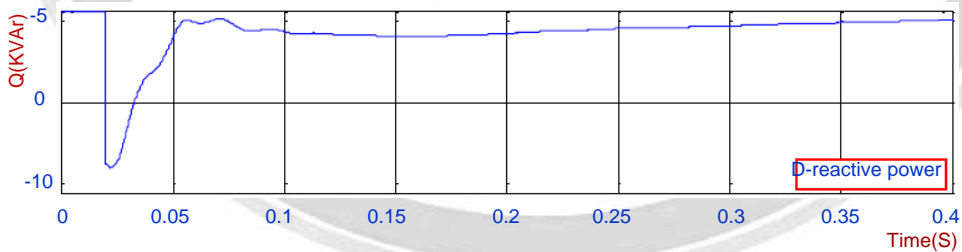
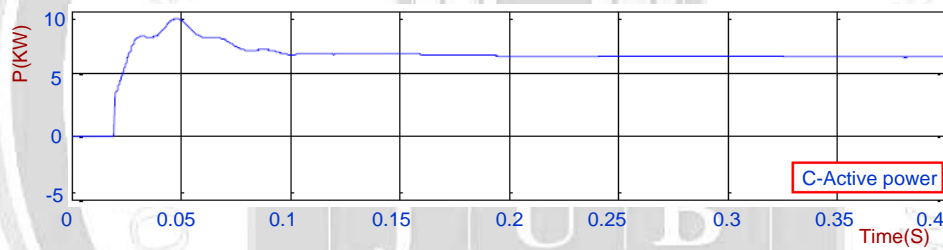
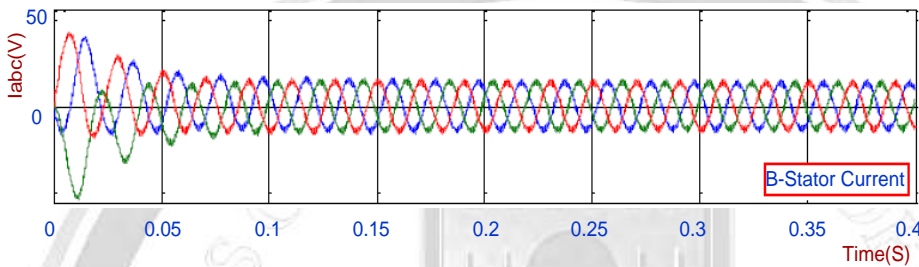
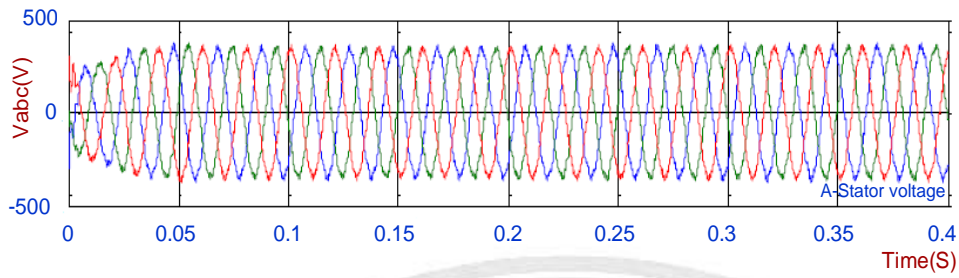
Figure (10). Current control loop of the GSC in S-domain [12].

8. Results and Discussion

This section is discussing the performance of the DFIG system under grid voltage fluctuations. The fluctuations are deliberated by varying the grid voltage values. The MatLab/SimuLink simulation is the tool used to analyze the system behavior for several cases of the grid disturbances. The wind speed and supply frequency changes on the system performance are taken in to consideration as well as the DFIG reactive power.

A- Simulation under balanced grid

The DFIG at steady state behavior waves are shown in Figure (11). The waveforms show that the DC link voltage is not changing as a result of control approach in the grid side converter while the reactive and active powers that the utility grid supplied are decoupled. The rotor and stator fluxes are not changing as shown in Fieger (16).



www.journalofbabylon.com | Journal.eng@uobabylon.edu.iq | ISSN: 2616 - 9916

ISSN: 2616 - 9916

www.journalofbabylon.com

Journal.eng@uobabylon.edu.iq

info@journalofbabylon.com

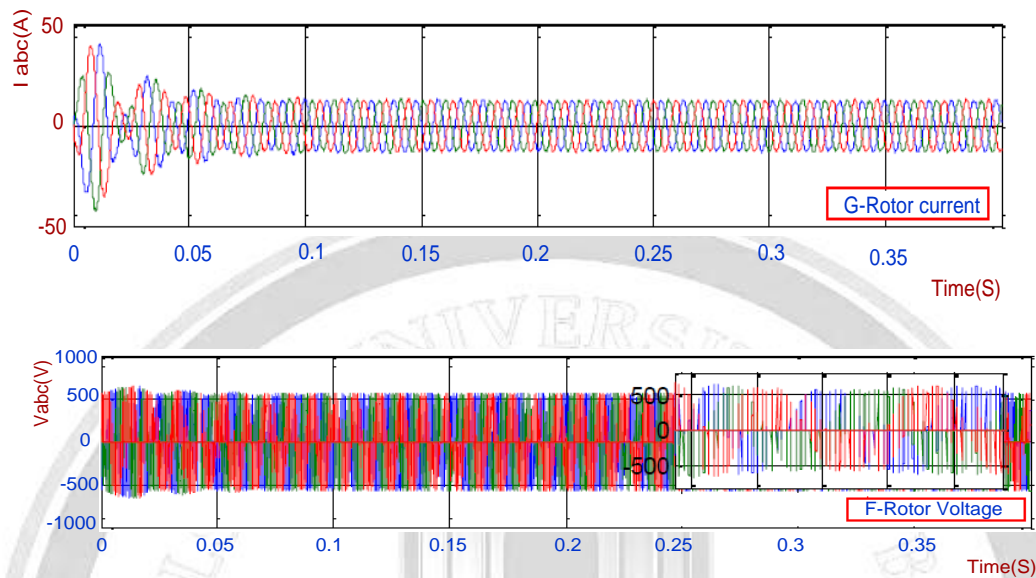
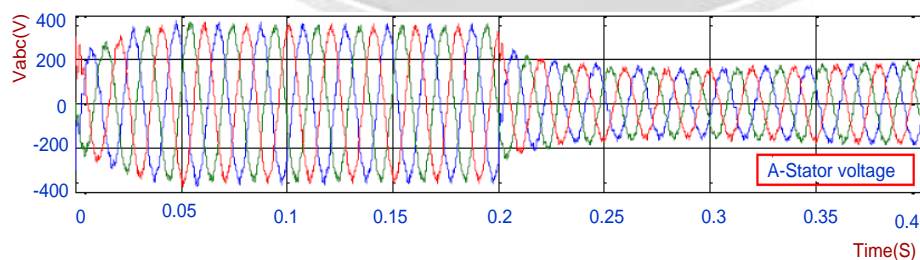
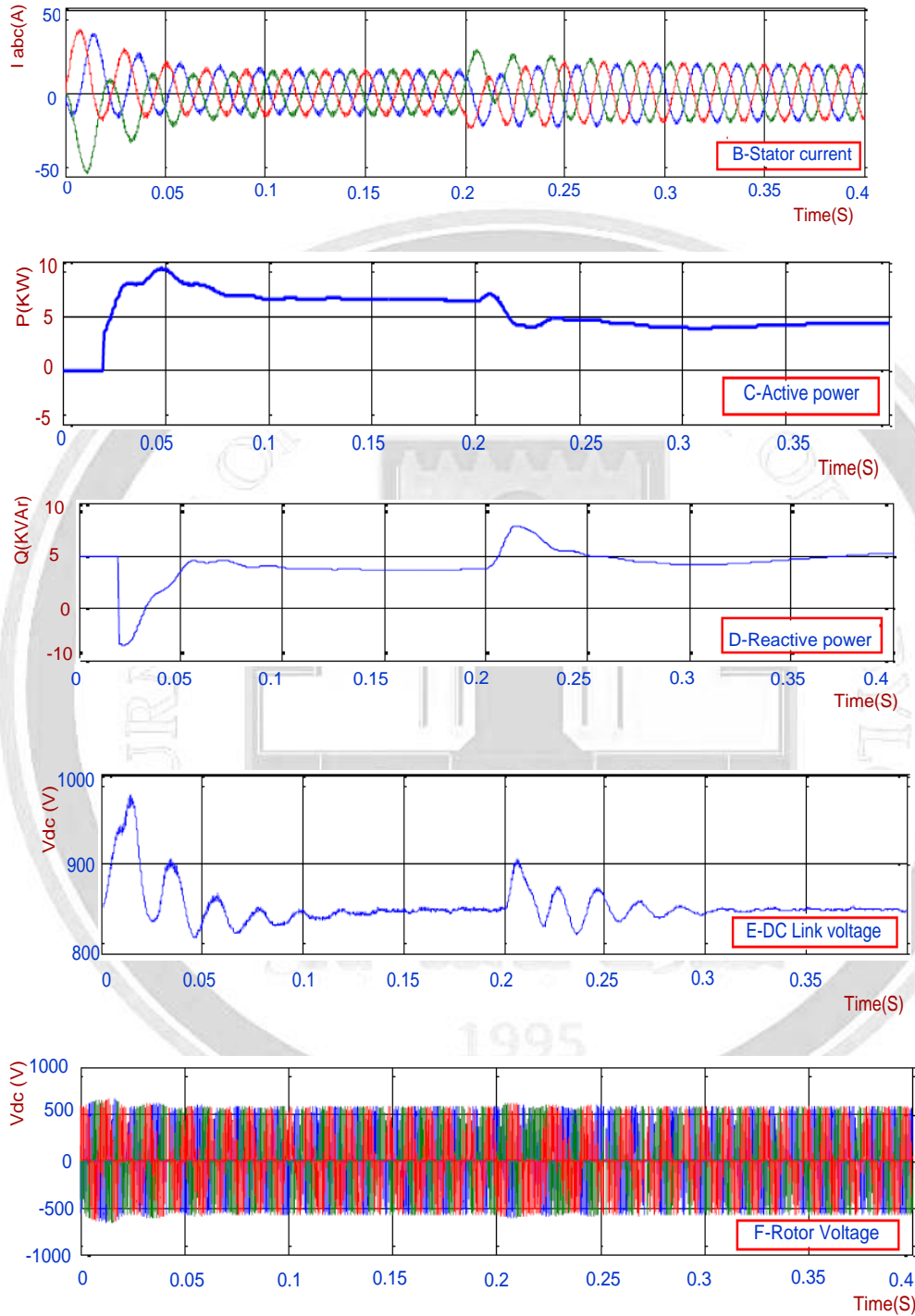


Fig (11) -Simulation under balanced grid

B- Simulation under Voltage Sag:

Figure (12) is a system simulation at voltage sag condition. The turbine maximum output mechanical power is reduced by generator electrical loss, at the DFIG system, is generating 7 kW as active power. At a sudden change in grid voltage from the rated value, say 415 V, the currents of the stator and rotor rises and P (active power) is unexpectedly fluctuates for a time to settle down to the rated value. The setting value of the reactive power is $0kV_{Ar}$. At voltage declines, a sudden increasing in a reactive power but the control protocol of the converter at the rotor side is bringing its back to its setting value ($0kV_{Ar}$). Through the converter at the grid, DC link voltage was set to 850 V. This voltage is also fluctuated at voltage sag then return to the setting value (850 V) despite that the rotor speed is kept not changing (1080 rpm) and the speed of wind also constant at 10 m/s. The rotor and converter outputs are having same values. It is showing that when the grid voltage is suddenly reduced to 50%, the rotor flux is reduced accordingly as shown in Fig (17).





www.journalofbabylon.com | Journal.eng@uobabylon.edu.iq | ISSN: 2616 - 9916

www.journalofbabylon.com | Journal.eng@uobabylon.edu.iq | ISSN: 2616 - 9916

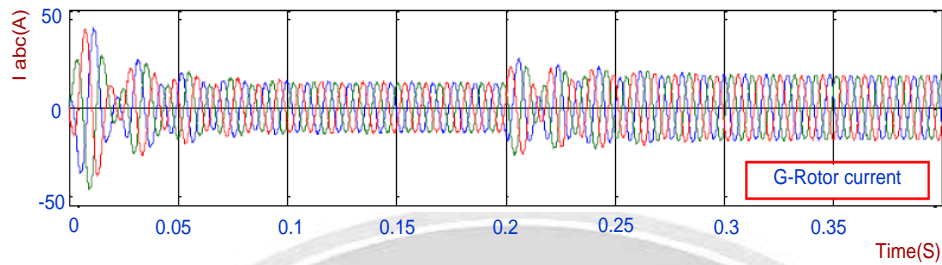
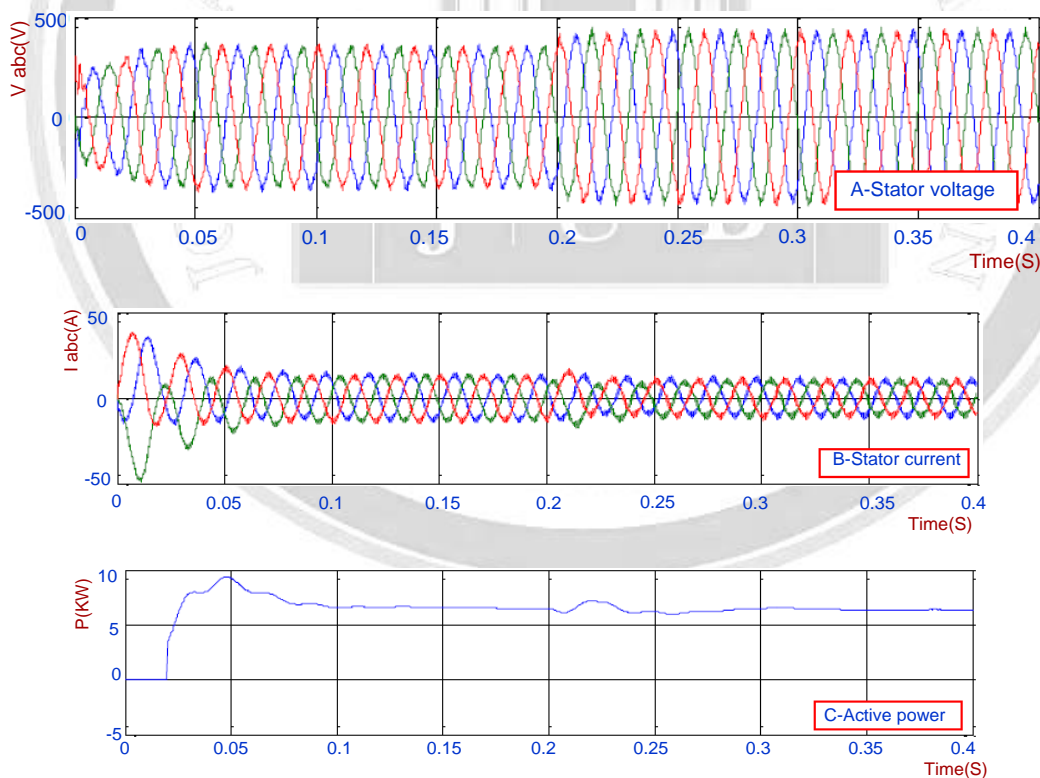


Fig (12) Simulation under Voltage sag:

C-Simulation under Voltage Swell

The simulation results of this case are clarified in Figure (13). At the 120% increase of the grid rated voltage, the results are showing that the rotor and stator currents are decreasing with a sudden decrease in the Q (reactive power) then back again to its zero value. The generator response at 0.2s at a voltage of 120% of the rated value. The rotor flux is also proportionally increasing with the voltage swell. As shown in Figure (18)



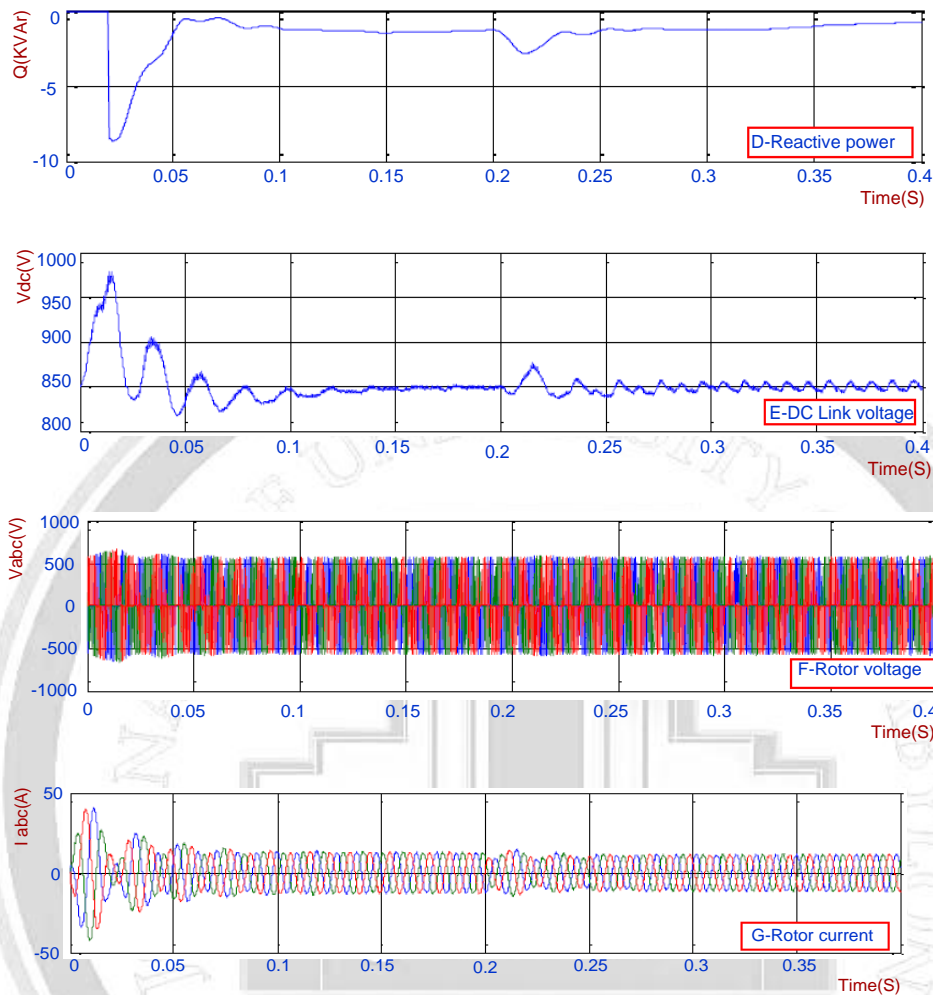
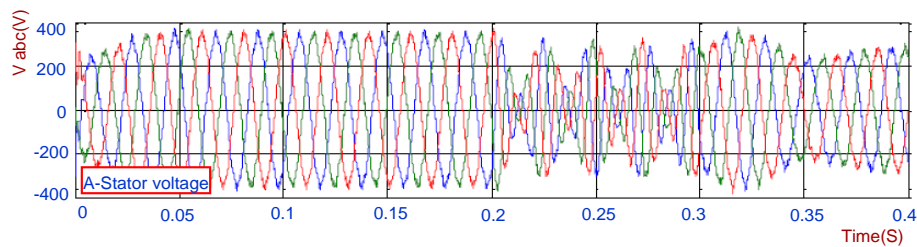


Fig (13).Simulation under Voltage swell

D. Simulation under Change in Supply Frequency

Figure (14) is showing the system response under the supply frequency changes (from rated frequency 50Hz to 48Hz). The machine response is out of control. When the supply frequency changed from 50Hz to 48Hz, the unexpected response of the machine could be observed in a time interval 0.22-0.3 seconds. This result is suggesting the use of different control protocol for this type of changes.



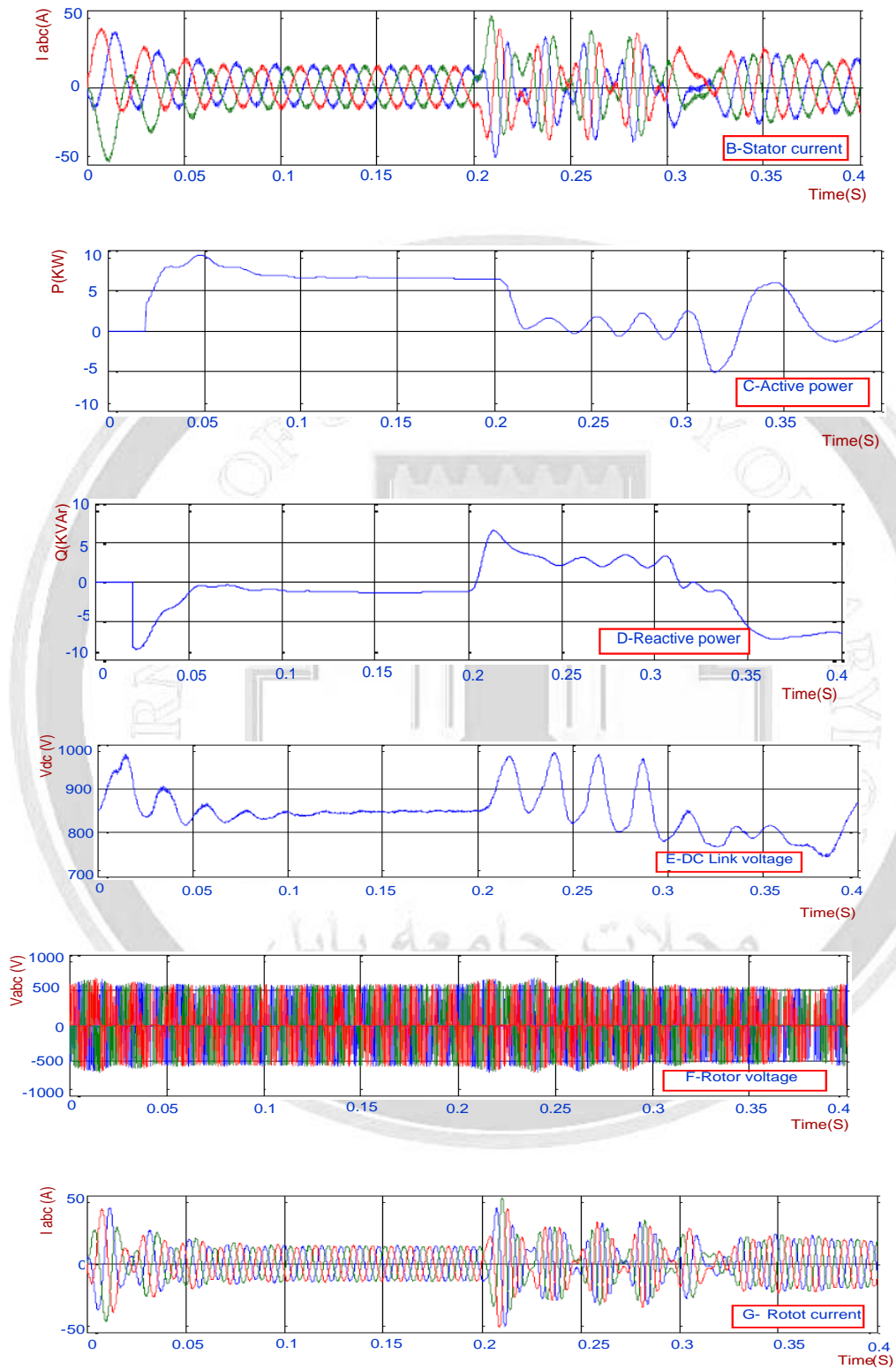
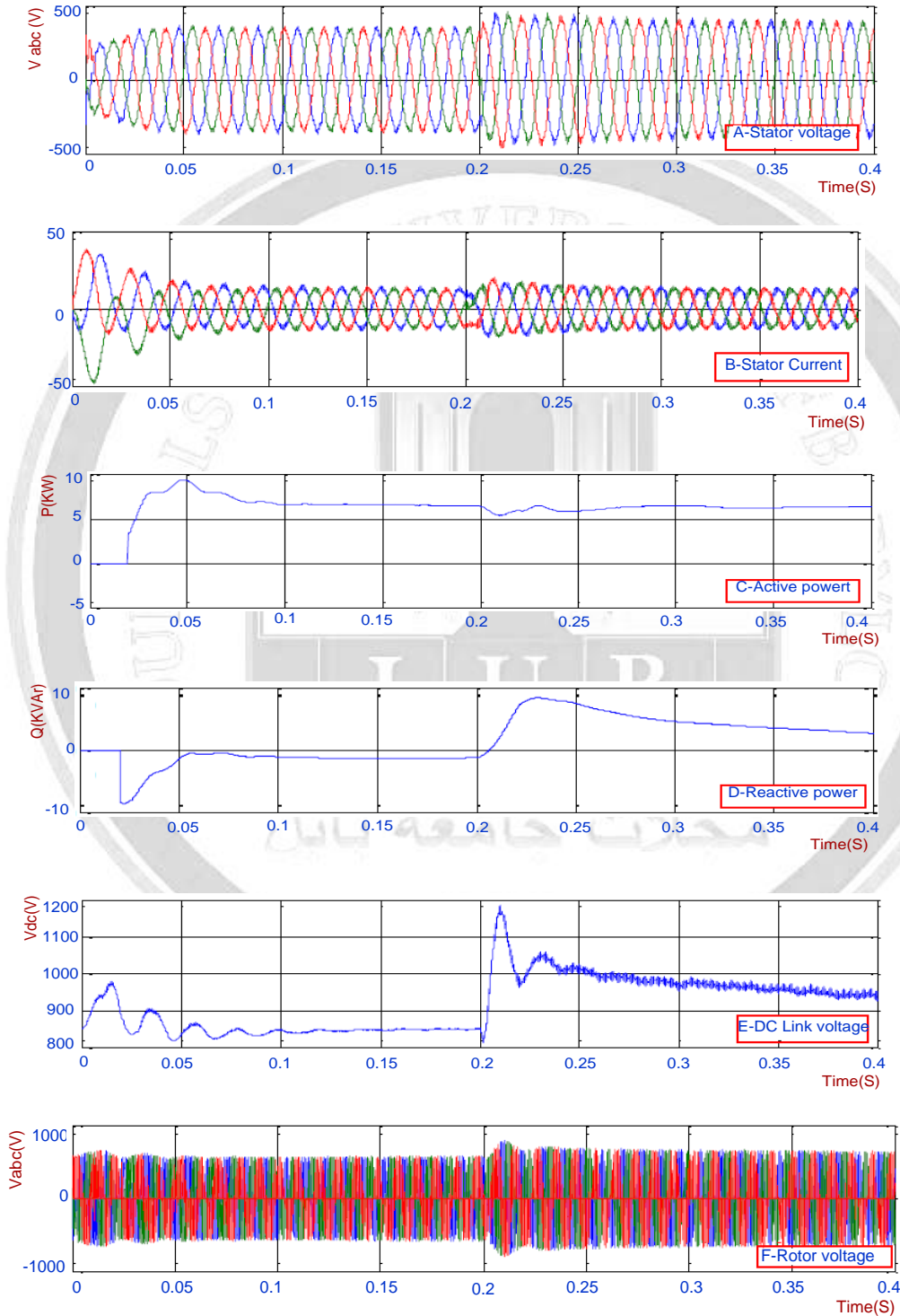


Fig (14).Simulation under change in supply frequency



E -Simulation under change in reactive power demand

Figure (15) shows the system parameters responses when the demand of the reactive power setting is changed from 0p.u. to 1p.u.



www.journalofbabylon.com

ISSN: 2616 - 9916

www.journalofbabylon.com

Journal.eng@uobabylon.edu.iq

info@journalofbabylon.com

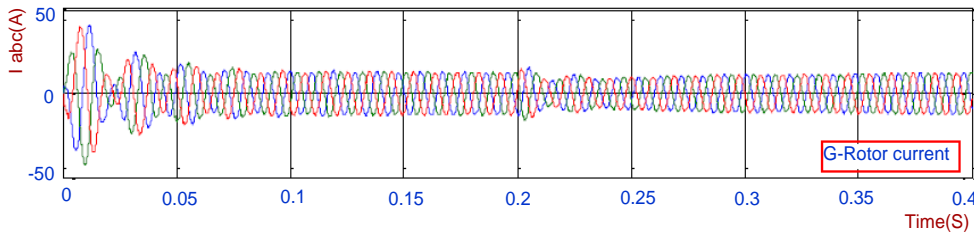
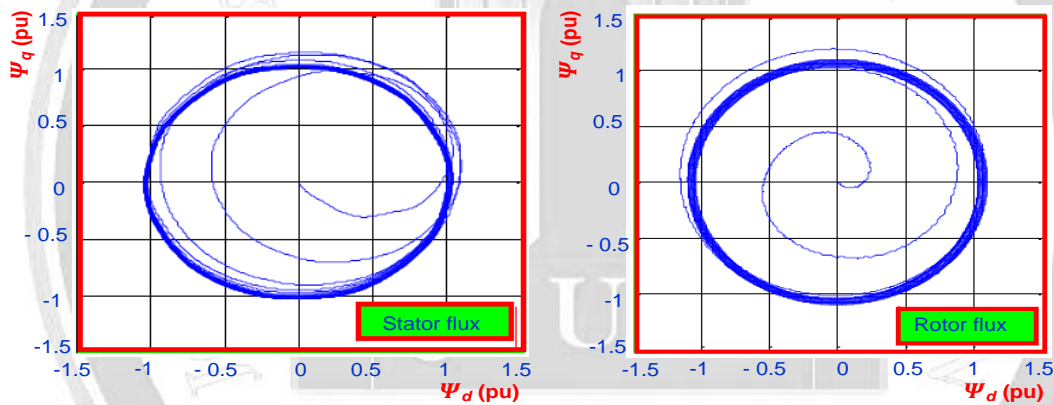


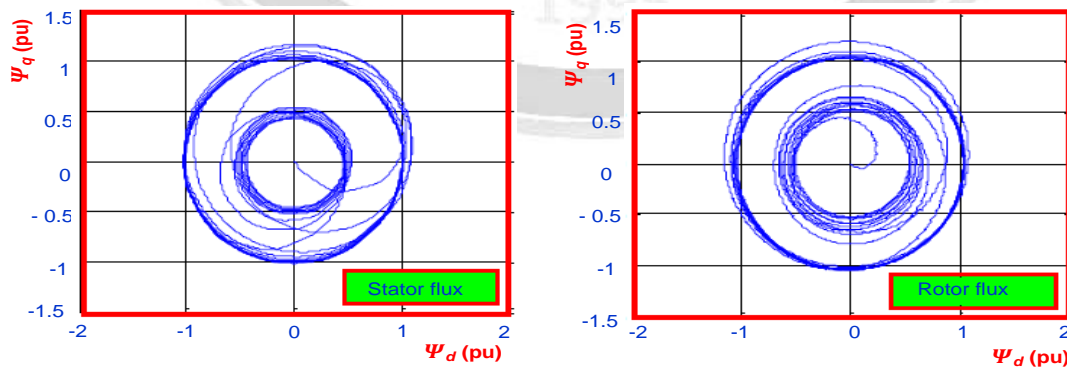
Fig (15) Simulation under change in reactive power demand

Figure 17 (a,b,c,d and d) is showing the Stator and Rotor Flux path under several cases. (balanced grid, Voltage Sag, Voltage Swell, Reactive power demand Conduction and change in Supply Frequency).

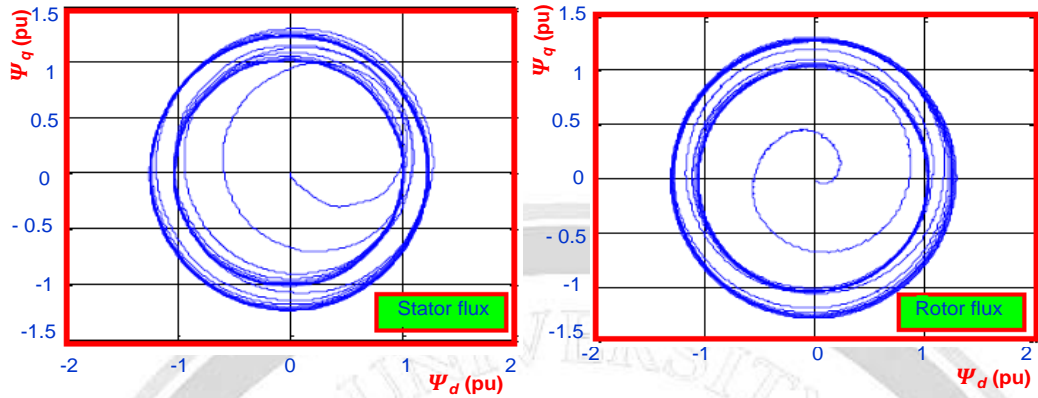
Under balanced grid the rotor and stator fluxes are not changing as shown in Figure (15-a) while It is showing that when the grid voltage is suddenly reduced to 50%, the rotor flux is reduced accordingly as shown in fig (15-b). The rotor flux is also proportionally increasing with the voltage swell as shown in Figure (15-c)



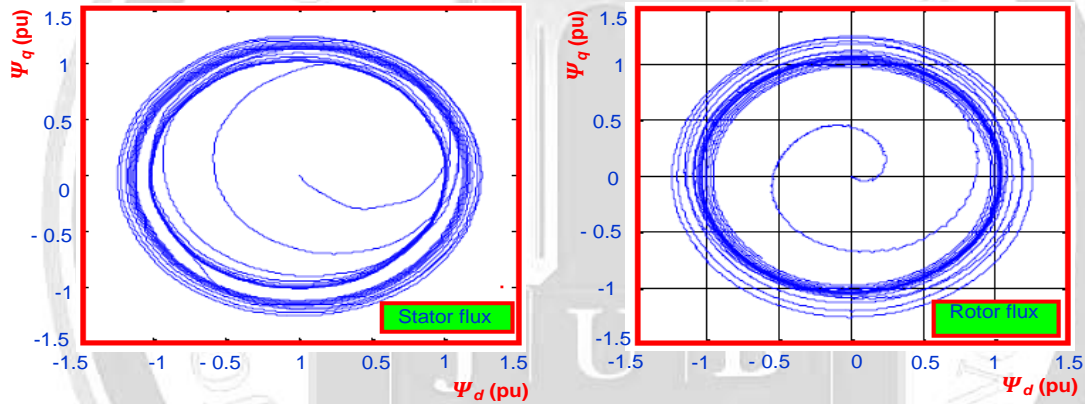
a. under balanced grid Conduction



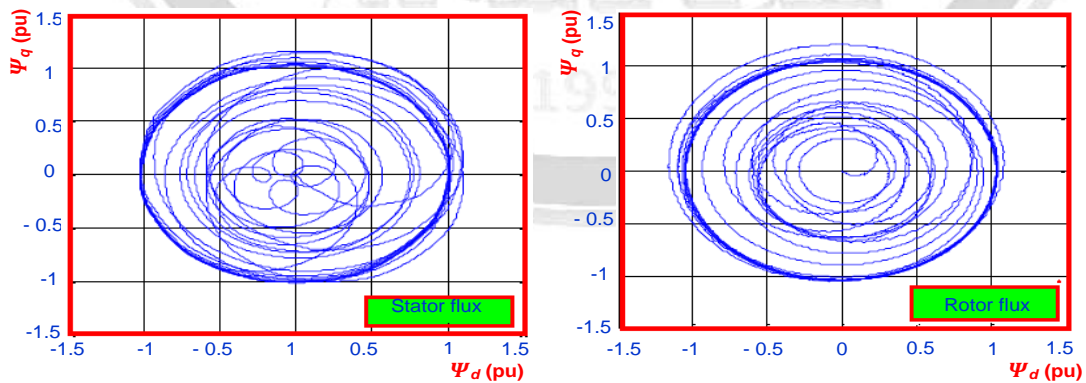
b. Under voltage sag Conduction



C. Under voltage swell Conduction



d. Under change in Reactive power



e. Under change in supply frequency

Finger (17). Stator and Rotor Flux path

مجله علمی مهندسی جوبس | Journal of University of Babylon for Engineering Sciences | Volume 29, No. 3, 2021

ISSN: 2616 - 9916

www.journalofbabylon.com

Journal.eng@uobabylon.edu.iq

info@journalofbabylon.com



10-Conclusions

The DFIG system's model is tested in a MATLAB/SIMULINK as a state space equations' system. The system with a back-to-back converter with a standard adjustment PI controller is also simulated. The conventional voltage control technique is used to control both grid side and machine side converters. The performance of this modeled DFIG system driven by wind turbine is analyzed under grid voltage fluctuation case. The test shows clearly the suitability of this controlling technique at the sudden changes in grid voltage. The results for different power quality issues have been obtained from the model at a selected switching frequency of 3 kHz and a dc-link capacitance of 1000 μ F.

11-References

- [1] "World Energy Outlook," International Energy Agencies, pp.303-338, 2010.
- [2] "Worldwide energy report," *Conf. World wind energy Renew. Energy Exhib.*, WWEA, Cairo, pp.6-8, 2010.
- [3] "Global wind Report: Annual market update," Global Wind Energy Council, pp.18-19, 2010.
- [4] A. D. Hansen, L. H. Hansen, "Market penetration of wind turbine concepts over the years," *European Wind Energy*, EWEA, vol. 10, pp. 81-97, 2007.
- [5] T. Ackermann, "Wind power in power systems," John Wiley and sons, England, 2005.
- [6] R. Pena, J. C. Clare, G. M. Asher, "Doubly fed induction generator using back-to-back PWM converters and its application to variable-speed wind-energy generation," *IEE Proc. Elect. Power Appl.*, vol. 143, no. 3, pp. 231-241, 1996.
- [7]. S. Alepuz R. Cardenas, R. Pena and G. Asher. Overview of control systems for the operation of dfig in wind energy applications. *IEEE Transactions on Industrial Electronic*, 60:2776{2796, July 2013.
- [8]. Lei, Y, Mullane, A., Lightbody G., Yacamini: "Modelling of the wind turbine with a doubly fed induction generator for grid integration studies" *IEEE Trans. Energy Convers*21(1), 257–264 (2006)
- [9]. Ibrahima Ngom, Alioune B Mboup"Efficient Control of Doubly Fed Induction Generator Wind Turbine Implementation in Matlab Simulink" *International Journal of Engineering Research and Applications*, 2248-9622, Vol. 8, Issue 7 (Part -I) July 2018, pp 06-12.
- [10] J.F. Manwell, J.G. McGowan, A.L. Rogers, "Wind Energy Explaine., Theory, Design and Application", John Wiley & Sons, LTD, 2003
- [11] M. Predescu¹, A.Bejinariu²" Influence of the Number of Blades on the Mechanical Power Curve of Wind Turbines" *International Conference on Renewable Energies and Power Quality Valencia (Spain)*, 15th to 17th April, 2009.
- [12]Roshen T. Ahmad" Modeling and Simulation of Wind Turbine Generator Using Matlab-Simulink *Journal of Al Rafidain University College*. ISSN (1681-6870) No. 40/2017
- [13]Othmane Zamzoum and , Youness El Mourabit"Active and Reactive Power Control of Wind Turbine based on Doubly Fed Induction Generator using Adaptive Sliding Mode Approach"(IJACSA) *International Journal of Advanced Computer Science and Applications*, Vol. 10, No. 2, 2019| P a g e 397-406 |
- [14] Othmane Zamzoum and , Youness , El Mourabit"Active and Reactive Power Control of Wind Turbine based on Doubly Fed Induction Generator using Adaptive Sliding Mode Approach"(IJACSA)



International Journal of Advanced Computer Science and Applications, Vol. 10, No. 2, 2019| Page 397-406

- [15] Karanam Deepak, Talari Aparna, A.Suresh Kumar, P Siva Deepthi: Simulation and Analysis of DFIG System with Wind Turbine Implementing Fuzzy Logic Control “ International Journal of Engineering and Advanced Technology (IJEAT) ISSN: 2249 – 8958, Volume-8 Issue-6, August 2019 .
- [16]Boumerid Bensahila and Med El Amine” Modeling, simulation and control of a doubly-fed induction generator for wind energy conversion systems” International Journal of Power Electronics and Drive System (IJPEDS) Vol. 11, No. 3, September 2020, pp. 1197~1210
- [17] A. Dendouga, R. Abdessemed, M. L. Bendaas and A. Chaiba, “Decoupled Active and Reactive Power Control of a Doubly-Fed Induction Generator (DFIG),” Mediterranean Conference on Control and Automation, Athens-Greece IEEE, 2007.
- [18]G. Yuan, C. Jianyun, Y. Li, "Vector Control and Synchronization of Doubly Fed Induction Wind Generator System," 2004 IPEMC Proceedings, pp. 886-890, 2004.
- [19] A. Petersson, T. Thiringer, L. Harnefors, T. Petru, "Modeling and Experimental Verification of Grid Interaction of a DFIG Wind Turbine," IEEE Trans. on Energy Conversion, vol. 20, No.4, pp. 878 886, 2005
- [20] L. Yazhou, M. Alan, L. Gordon and Y. Robert "Modeling of the Wind Turbine with a Doubly Fed Induction Generator for Grid Integration Studies", IEEE Transactions on Energy Conversion, vol. 21, no. 1, pp. 257-264, 2006.
- [21] F. El Aamri, H. Maker, D. Sera and al, “A Direct Maximum Power Point Tracking Method for Single-Phase Grid-Connected PV Inverters,” IEEE Transactions on Power Electronics, vol. 33, 2018.
- [22]Li, W.; Chao, P.; Liang, X.; Sun, Y.; Qi, J.; Chang, X. Modeling of complete fault ride-through processes for DFIG-Based wind turbines. *Renew. Energy* 2018, 118, 1001–1014.
- [23]Precup, R.; Kamal, T.; Hassan, S.Z. *Advanced Control and Optimization Paradigms for Wind Energy Systems*; Springer: Singapore, 2019; ISBN 978-981-13-5994-1.

مجلات جامعة بابل
1995



نمذجة ومحاكاة وتحليل المولد الحثي ذو التغذية المزدوجة لتوربينات الرياح تحت تذبذب جهد الشبكة

١- كرار محمد الانباري ٢- حيدر حسين كاظم ٣- عبد الرسول عبيد الحيدر

قسم الهندسة الكهربائية، جامعة بابل، العراق

Karrar139@yahoo.com eng.hayder.kadhumi@uobabylon.edu.iq Ajwadi.haydari@gmail.com

Corresponding Author : eng.hayder.kadhumi@uobabylon.edu.iq

الخلاصة

لغرض ضمان أفضل حالة تشغيل لتوربينات الرياح في ظل الظروف الحرجة، من الضروري إجراء تحليل شامل لعناصر تحكم المحول في كل من جانبي الماكينة والشبكة. يلعب جانب الشبكة دوراً رئيسياً، لذلك يجب تلبية متطلباته مثل التثبيت، وتجاوز الأخطاء، وتحسين جودة الطاقة، والمزامنة، والتحكم في الطاقة، والمتطلبات الأخرى. تهدف هذه الورقة إلى تحليل المولد الحثي ذو التغذية المزدوجة (DFIG). يجب أن يغطي التحليل الحالات التالية: تحت الشبكة المتوازنة، ترهل الجهد، تضخم الجهد، والتغيرات في الطلب على الطاقة التفاعلية وتحت التغيرات في تردد المصدر. هناك حاجة إلى نموذج لغرض تحليل والتحكم في لمولد الحثي ذو التغذية المزدوجة بأكمله في عمليات الحالة المستقرة والحالة العابرة. يتم استخدام محولات ظهر إلى ظهر في هذا النظام. يتم إنشاء نموذج لمحول الشبكة الذي يتحكم بشكل مستقل في الطاقة النشطة والمتفاعلة بما في ذلك جهد وصلة التيار المستمر. تم تصميم نموذج المحول الجانبي للآلة أيضاً بحيث يحافظ على عامل الطاقة الموحد ويتحكم في الطاقة التفاعلية بغض النظر عن الحالة العابرة للشبكة. تم استخدام MATLAB / SIMULINK لهذا التحليل

الكلمات الدالة: - المولد الحثي ذو التغذية المزدوجة (DFIG)، النمذجة والمحاكاة والتحليل.

مجلات جامعة بابل
1995